Anal. Chem. **2010,** *82,* 543–547

Femto Liquid Chromatography with Attoliter Sample Separation in the Extended Nanospace Channel

Masaru Kato,[†,‡,||] Masanori Inaba,[†] Takehiko Tsukahara,[†,⊥] Kazuma Mawatari,[§] Akihide Hibara,[†,#] and Takehiko Kitamori*[,†,‡,§]

Department of Applied Chemistry, Graduate School of Engineering, and Center for NanoBio Integration (CNBI), The University of Tokyo, 7-3-1 Hongo, Bunkyo-ku, Tokyo 113-8656, and Japan, Kanagawa Academy of Science, 3-2-1 Sakado, Takatsu, Kawasaki, Kanagawa 213-0012, Japan

A liquid chromatography system, comprising a separation column with a width and depth of a few hundred nanometers, was fabricated on a glass microchip (femto liquid chromatography, fLC). The size of this system was approximately 10^{11} times smaller than that of a conventional LC system, the flow rate was subpicoliter/minute, and the injection volume was a few hundred attoliters. The fLC system did not require packing stationary phase and was capable of separating solutes with different molecular charges (fluorescein and sulforhodamine B) that could not be separated on a conventional LC column whose surface was covered with the same functional group as that of the column of the fLC system. The fLC system represented herein overcomes limitations of conventional chromatography separation, namely, heterogeneity of the stationary phases and eddy diffusion. Scale-down of the chromatography system brought advantages not only in reduction of sample volume but also in separation efficiency. The fLC system can analyze a very small amount of sample with high efficiency and will be useful in analyzing small samples, such as single cells and synaptic clefts. fLC greatly influences and benefits various fields such as life sciences, medicine, environmental science, and manufacturing by the improvement of separation technology.

The 10^1 to 10^2 nm scale space (extended nanospace) is a promising experimental area for implementing highly integrated micro/nanofluidic devices and for better understanding molecular physical chemistry.[1] Characteristics of the extended nanospace include a large interfacial area to volume ratio and a substantial effect on the electric potential gradient arising from the electric double layer.[2,3] We previously reported that the properties of water in the extended nanospace were altered, displaying higher viscosity, a lower dielectric constant, slower translational motion, and higher proton mobility.[4,5]

Liquid chromatography is one of the most popular separation techniques attempted on fabricated chromatography microchips.[6,7] Although improvements in separation efficiency and detection limits are realized by the miniaturization of the high-performance liquid chromatograph (HPLC),[8] it is difficult to control fluid flow rates at very small volumes to fit the miniaturized HPLC. State-of-the-art HPLC, called "nanochromatography", controls fluid with an accuracy of several hundred nanoliters per minute and supports numerous discoveries in the life science field, etc.[9,10] Chromatography systems operating on the microscale face considerable technical difficulties in packing the stationary phase in the separation channel with high reproducibility and accuracy. This problem can be overcome by reduction of the channel size to a few hundred nanometers, resulting in an interfacial area to volume ratio of the extended nanospace channel similar to that of a conventional HPLC column. Therefore, an extended nanospace channel without packing material could be used as a separation column. This would remove limitations of current LC systems, namely, the generation of heterogeneous pathways for the solute (eddy diffusion) and resultant peak broadening. Furthermore, unique properties of the extended nanospace mentioned above would be advantageous for chromatographic separations. Hence, the use of nanospace represents a novel technique in the field of chromatographic separation. In fact, it was predicted theoretically

* To whom correspondence should be addressed. E-mail: kitamori@icl.t.u-tokyo.ac.jp.

† Graduate School of Engineering, The University of Tokyo.

‡ Center for NanoBio Integration, The University of Tokyo.

§ Kanagawa Academy of Science.

|| Present address: Graduate School of Pharmaceutical Sciences and Global COE Program, The University of Tokyo, 7-3-1 Hongo, Bunkyo-ku, Tokyo 113-0033, Japan.

⊥ Present address: Research Laboratory for Nuclear Reactors, Tokyo Institute of Technology, 2-12-1 Ookayama, Meguro-ku, Tokyo 152-8550, Japan.

Present address: Institute of Industrial Sciences, The University of Tokyo, 4-6-1 Komaba Meguro-Ku, Tokyo 153-8505, Japan.

(1) Hibara, A.; Tsukahara, T.; Kitamori, T. *J. Chromatogr., A* **2009**, *1216*, 673–683.
(2) Pu, Q.; Yun, J.; Temkin, H.; Liu, S. *Nano Lett.* **2004**, *4*, 1099–1103.
(3) Abgrall, P.; Nguyen, N. T. *Anal. Chem.* **2008**, *80*, 2326–2341.
(4) Hibara, A.; Saito, T.; Kim, H.-B.; Tokeshi, M.; Ooi, T.; Nakao, M.; Kitamori, T. *Anal. Chem.* **2002**, *74*, 6170–6176.
(5) Tsukahara, T.; Hibara, A.; Ikeda, Y.; Kitamori, T. *Angew. Chem., Int. Ed.* **2007**, *46*, 1180–1183.
(6) Ericson, C.; Holm, J.; Ericson, T.; Hjerten, S. *Anal. Chem.* **2000**, *72*, 81–87.
(7) Throckmorton, D. J.; Shepodd, T. J.; Singh, A. K. *Anal. Chem.* **2002**, *74*, 784–789.
(8) Saito, Y.; Jinno, K.; Greibrokk, T. *J. Sep. Sci.* **2004**, *27*, 1379–1390.
(9) Shen, Y. F.; Zhao, R.; Berger, S. J.; Anderson, G. A.; Rodriguez, N.; Smith, R. D. *Anal. Chem.* **2002**, *74*, 4235–4249.
(10) Kitajima, T. S.; Sakuno, T.; Ishiguro, K.; Iemura, S.; Natsume, T.; Kawashima, S. A.; Watanabe, Y. *Nature* **2006**, *441*, 46–52.

10.1021/ac9017605 © 2010 American Chemical Society
Published on Web 12/23/2009

that solutes with different charges will separate efficiently by passing through the extended nanospace channel using only pressure-driven water flow as the mobile phase. In the channel, the effect of the electric potential was considerable, and an electric potential gradient was observed in most areas of the channel. The gradient produced the localization of solutes based on charge where differences existed in velocities. The flow profile in the channel was parabolic, with the flow rate at the center faster than that near the wall. Nevertheless, experimental proof of this prediction has yet to be obtained in the space of less than 1 μm.[11−13]

Here we describe a new LC with a flow rate of several hundred femtoliters per minute, femto liquid chromatography (fLC). The fLC system overcomes limitations of conventional chromatography separation utilizing the extended nanospace.

EXPERIMENTAL SECTION

Microchip Fabrication. The extended nanospace channels were fabricated on high-purity synthetic quartz glass substrates with impurities at less than 1 ppb (VIOSIL-SX, Shin-Etsu Quartz Co., Ltd., Tokyo, Japan) by electron-beam lithography and plasma etching. All fabricated spaces had widths (W) of 110−910 nm and depths (D) of 170−650 nm. The substrate fabricated with channels was thermally laminated with a coverplate in a vacuum furnace at 1080 °C. Ultrapure water was obtained using a water purification system composed of a reverse osmosis membrane, an ion-exchange cylinder, and a UV sterilizer (Millipore, Bedford, MA) and had a specific resistivity greater than 18.0 MΩ·cm. Dust and impurities were excluded by performing all operations in class-100 and -1000 clean rooms. The sizes of the extended nanospace channels used in this study were 110 × 170, 270 × 280, 430 × 420, 830 × 650, and 1200 × 1200 nm^2 (width × depth).

Setup of the fLC System. Figure 1a shows a photograph and schematic of the microchip used in the present study. The microchip was embedded in an aluminum chip holder (ICH-01K, IMT, Kawasaki, Kanagawa, Japan), and PEEK tubes (100 μm i.d., Upchurch Scientific, Oak Harbor, WA) were connected to the inlet and outlet of the microchannels with Teflon joints (0.6, Nihon Seimitsu Kagaku Co., Ltd., Tokyo, Japan), O-rings (AS568-001, Air Water Mach Inc., Matsumoto, Nagano, Japan), and Araldite rapid epoxy-based glue (Huntsman, Salt Lake City, UT). The microchip possesses four U-shaped microchannels (width, 200 μm; depth, 8 μm), three parallel extended nanospace channels, and one orthogonal extended nanospace channel (Figure 1c). Three parallel extended nanospace channels were used to increase the fluorescence signal of the solute, as the volume of the extended nanospace channel was very small and the signal from a single channel was very low. The signal intensities and velocities of solutes were the same in all of the extended nanospace channels used. Both ends of these extended nanospace channels were connected to microchannels in order to introduce the sample and the elution solvents (Figure 1b).

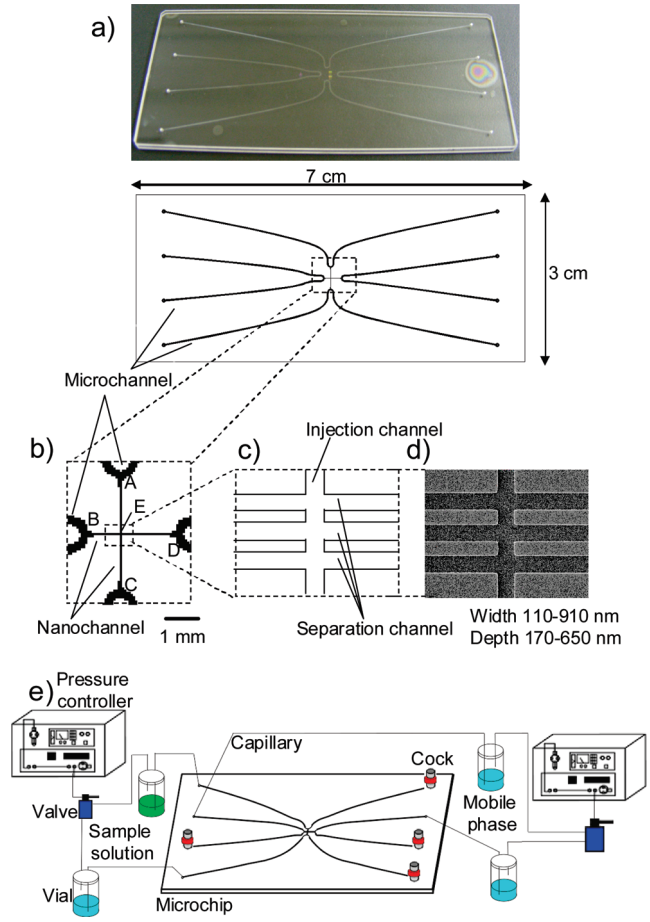

Figure 1. (a) Photograph and schematic of a microchip with an extended nanospace channel. (b) Enlarged view of the connection between the microchannel and extended nanospace channel on the fabricated microchip. (c) Enlarged cross-sectional view of the extended nanospace channels. (d) SEM image of the cross sections of the extended nanospace channels. (e) Schematic illustration of the air pressure based fLC system. The distances between A and E, B and E, C and E, and D and E are 1.6, 0.8, 1.6, and 1.6 mm, respectively.

To achieve femtoliter-scale liquid control, the pressure controller shown in Figure 1e was used.[14] Control of the flow rate in the extended nanospace channel is difficult due to large back pressure and small volume. To adjust the back pressure in the extended nanospace channels, the lengths of the channels (between A and E, C and E, and D and E in Figure 1b) were the same (1.6 mm). The sample solution was poured into a vial possessing two gateways. The outlet was connected by a capillary tube to one of the microchannels on the chip, and the inlet was connected through $^1/_{16}$ in. stainless steel tubing to one of the air pressure controllers (PC20, Nagano Keiki Co., Ltd., Tokyo, Japan). Air was pressurized into the sample solution from the inlet using the air pressure controller, and the sample solution in the sample vial was delivered to one side of the microchannel from the outlet of the vial. After the stopcock connected to the other side of this microchannel was closed, the sample solution inside the microchannel could be introduced into the extended nanospace channel via pressure-driven flow. In this system, the pressures in the microchannel and extended nanospace chan-

(11) Pennathur, S.; Santiago, J. G. *Anal. Chem.* **2005**, *77*, 6772–6781.
(12) Griffiths, S. K.; Nilson, R. H. *Anal. Chem.* **2006**, *78*, 8134–8141.
(13) Wang, X.; Wang, S.; Veerappan, V.; Byun, C. K.; Nguyen, H.; Gendhar, B.; Allen, R. D.; Liu, S. *Anal. Chem.* **2008**, *80*, 5583–5589.
(14) Tsukahara, T.; Mawatari, K.; Hibara, A.; Kitamori, T. *Anal. Bioanal. Chem.* **2008**, *391*, 2745–2752.

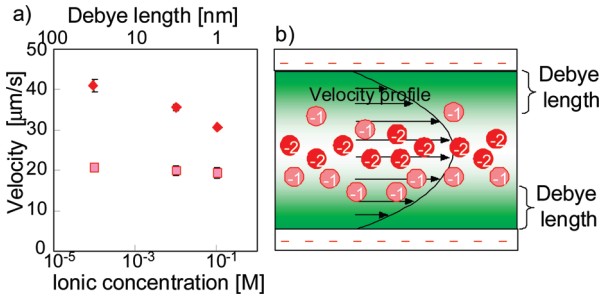

Figure 2. (a) Effect of ionic concentration (Debye length) on the velocities of solutes with different charges. The measurement was performed more than nine times in each data point. (b) Schematic illustration of the distribution of solutes and their velocity profile in the extended nanospace channel. The symbols ◆ (red) and ■ (pink) represent fluorescein (−2) and sulforhodamine B (−1), respectively. The number in parentheses and in the circle indicate the charge of the solute.

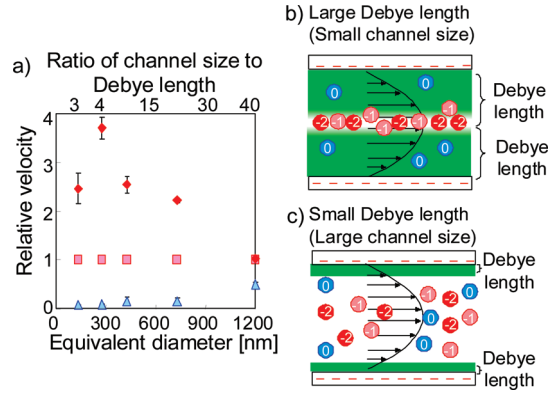

Figure 3. (a) Effect of channel size on the velocities of solutes. The measurement was performed more than nine times at each data point. Schematic image of the distribution of solutes with different charges in a channel with (b) high aspect ratio and (c) low aspect ratio. The symbols ◆ (red), ■ (pink), and ▲ (light blue) represent fluorescein (−2), sulforhodamine B (−1), and rhodamine B (0), respectively. The number in parentheses and in the circle indicate the charge of the solute.

nel were kept constant. The pressure was controlled by the air pressure controllers to an accuracy of ±0.001 MPa. The maximum pressure of our fLC system was approximately 1 MPa.

Velocity Measurement and Separation Study. The microchip was placed on the motorized stage (BIOS 105T, Sigma Kouki Co., Ltd., Tokyo, Japan) of a fluorescence microscope, model IX70 (Olympus, Tokyo, Japan). A CCD camera (ImagEM, Hamamatsu, Shizuoka, Japan) was used to detect the fluorescence signal, and software (Aquacosmos, Hamamatsu) was used for the analysis. Velocities were calculated by the delay of the fluorescence signal change between the two remote positions.

A pressure of 80 (B in Figure 1b), 80 (D in Figure 1b), 100 (A in Figure 1b), and 0 (C in Figure 1b) kPa was applied when the sample was introduced. Pressure of 150 kPa was applied only to B in Figure 1b, while the remaining channels were left unpressurized during separation.

Conventional HPLC Study. The HPLC system consisted of a model L-6200 liquid chromatograph (Hitachi, Tokyo, Japan), a Rheodyne injector, a micro21FP-01 (JASCO, Tokyo, Japan), and a smart chrom data converter (KYA Technology, Tokyo, Japan). We chose Inertsil SIL 100A 5 μm (GL science, Tokyo, Japan) as the separation column (4.6 mm i.d. × 150 mm) packed with silica particles covered with silanol groups (Si−OH), the same functional group as that on the extended nanospace channel surface. Phosphate buffer (0.1 mM, pH 8) was used as the mobile phase, and the flow rate was 1.0 mL min^{-1}. Fluorescence was monitored at 550 nm, and excitation was monitored at 505 nm.

RESULTS AND DISCUSSION

Effect of Electric Double Layer. First, we examined the effect of the electric double layer on the velocity of a solute in the extended nanospace channel using pressure-driven flow. The size of the electric double layer (Debye length) was determined by the ionic concentration of the mobile phase. The Debye length was estimated at 30, 3, and 1 nm when the ionic concentration was 10^{-4}, 10^{-2}, and 10^{-1} M, respectively. Velocities of 50 μM fluorescein and sulforhodamine B in phosphate buffer (pH 8) were measured using a 270 × 280 nm^2 channel (Figure 2a). An increase in the ionic concentration brought a decrease in velocities of both solutes and a reduction of their difference. This result showed that the size of the electric double layer in the nanospace channel has a significant effect on the velocity of the solute and presumably arises from the localization of solutes in the channel.[15] The effect of the electric potential was large, and the electric potential gradient was observed in most areas of the channel. This gradient produced a localization of the solutes based on their charge where differences existed in velocities (Figure 2b). In the extended nanospace channel, the flow profile was parabolic, with the flow rate at the center faster than that near the wall.[16] Therefore, the more negatively charged solute had higher velocity because it localized to the center of the channel. Although the Debye length was about 1 nm, when the ionic concentration was 10^{-1} M, the velocity of fluorescein was slightly faster than that of sulforhodamine B, even though both are negatively charged and experience electrostatic repulsion from the wall. It is supposed that the 1 nm Debye length was too small to produce a velocity difference in the solutes when compared with the channel size (270 nm). It is probable that other factors, such as electrostatic interaction with surface charge or a unique property of water in the extended nanospace, were involved in inducing this small velocity difference between the solutes under these conditions.

Effect of Channel Size. Next, we examined the effect of channel size on the velocities of the solutes. The shape of the channels had a near-unity aspect ratio, and the equivalent diameters of these channels were 135, 275, 425, 730, and 1200 nm. The equivalent diameter (D_e) was defined from the depth (d) and width (w) of the channel by the following equation: $D_e = 2dw/(d + w)$. The velocity of sulforhodamine B was used as a standard, and the ratio of the velocity of the solutes to that of sulforhodamine B is shown in Figure 3a. The velocity of rhodamine B was the lowest of the three solutes, and the velocities of sulforhodamine B and fluorescein (in order of increasing speed) were higher in all the channels. This order was converse to the charge value of each solute. Although the velocity difference of

(15) Williams, S. K. R.; Lee, D. *J. Sep. Sci.* **2006**, *29*, 1720–1732.
(16) van der Heyden, F. H. J.; Stein, D.; Dekker, C. *Phys. Rev. Lett.* **2005**, *95*, 116104.

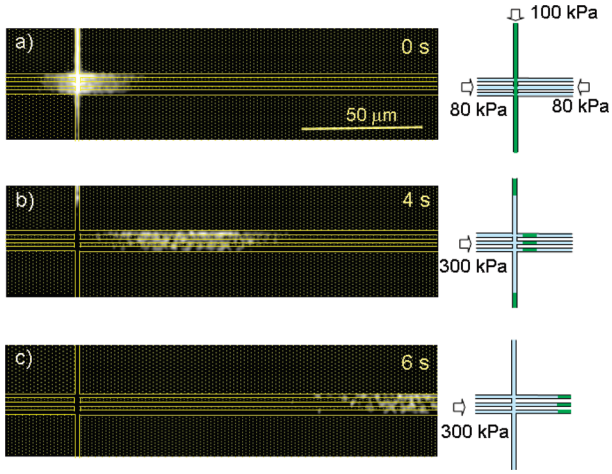

Figure 4. Fluoresence (left) and schematic (right) images of attoliter sample injection at different times after injection: (a) 0, (b) 4, and (c) 6 s. Yellow lines indicate extended nanospace channels. Green and light blue indicate sample solution and mobile phase, respectively.

the negatively charged solutes, fluorescein and sulforhodamine B, was very small in the microspace, when the channel surface was covered with negative charges, a clear velocity difference was observed in the extended nanospace channel. The velocity difference between fluorescein and sulforhodamine B decreased when the channel size became larger or smaller than 270 nm, and the velocities of both were almost the same when the channel size was 1200 nm. If the electrostatic interaction between the channel surface and solutes is the major source of the velocity difference, the difference should become larger as the channel size becomes smaller. However, the velocity difference was maximized when the channel size was about 270 nm. Therefore, electrostatic interactions are not the major reason for the velocity differences. The Debye length was about 30 nm in this condition, and the largest velocity difference was obtained when the ratio of channel size to the Debye length was about 4. This value is similar to that predicted theoretically.[17,18] When the Debye length is too large compared to the area of the channel, negatively charged solutes localize to the channel center, and it is hard to obtain velocity differences for the solutes (Figure 3b). On the contrary, if the Debye length is too small compared to the area of the channel, negatively charged solutes spread throughout the channel, and there is no difference in their velocities (Figure 3c). These results indicate that the electric double layer induced localization of the solutes and that this localization caused the velocity differences between the solutes. This phenomenon was emphasized when the channel diameter was less than 1 μm. Therefore, the electric double layer induced a velocity difference between the solutes in the extended nanospace channel that was scarcely evident in the microchannel.

Sample Injection. Next, we attempted to inject two different solutes into the extended nanospace channel. Figure 4 shows microscope images of a fluorescence solute injected into the separation channel. The microchip had one perpendicular channel for sample injection and three horizontal channels for separation (Figure 1, parts c and d). The fluorescence signal from the sample moved in the loading channel from the top to the bottom, and

(17) Xuan, X.; Li, D. *Electrophoresis* **2007**, *28*, 627–634.
(18) Xuan, X. *Anal. Chem.* **2007**, *79*, 7928–7932.

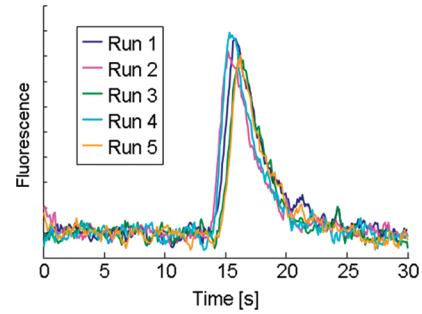

Figure 5. Reproducibility of the chromatograms (five repeated analyses). Conditions: mobile phase, 0.1 mM phosphate buffer (pH 8); sample, 60 mM sulforhodamine B.

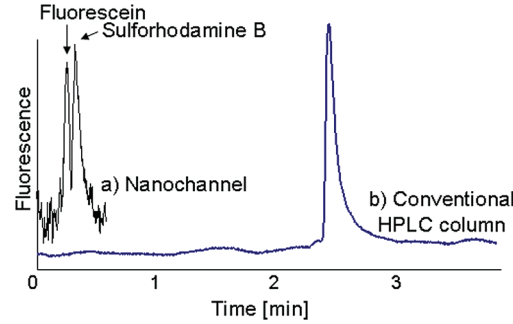

Figure 6. Chromatograms of fluorescein and sulforhodamine B from (a) an extended nanospace channel and (b) a conventional HPLC column. Conditions: mobile phase, 0.1 mM phosphate buffer (pH 8); column, Inertsil SIL 100A 5 μm (4.6 mm i.d. $\times$ 150 mm); flow rate (a) 490 fL min^{-1}, (b) 1.0 mL min^{-1}; detection, fluoresence Ex. 505 nm, Em. 550 nm.

then the applied pressure was changed (Figure 4a). The fluorescence signal was also obtained around the channel because the fluorescence signal was transmitted through the glass plate. The solutes in the cross section (volume of the section was approximately 230 aL) were injected into the separation channel and separated as the solutes moved from left to right in the separation channel (Figure 4, parts b and c). The relative standard deviation of repeatability of the injection volume was less than 5% (Figure 5), which was acceptable for further analysis. The repeatability of the chromatography system was satisfactory (Figure 5). Such excellent repeatabilities of the injection volume and elution time have not been previously reported for a nano separation system. These results indicate that this injection system would be suitable for an fLC system.

Separation of Solutes with Different Charges. Finally, we tried to separate solutes with different charges (fluorescein and sulforhodamine B) using a 328 nm channel. On a conventional HPLC column whose surface was covered with silanol group, both solutes eluted around 2.5 min and were not separated. This result was supported by our data in Figure 3a confirming that these solutes could not separate when the channel size becomes large. Although the surface of both the extended nanospace channel and the conventional column were covered with silanol groups, these solutes were separated only in the extended nanospace channel. Figure 6 shows the chromatogram obtained 1200 μm downstream from the injection point. Adequate separation was obtained using 0.1 mM phosphate buffer (pH 8) as the mobile phase. Fluorescein and sulforhodamine B separated well within 30 s, and the elution time of fluorescein was faster than that of

sulforhodamine B. The theoretical plate numbers of fluorescein and sulforhodamine B were 210 and 206, respectively. The plate heights were 5.7 and 5.8 μm, respectively. Although the data for plate height are only several times smaller compared with a conventional column, sample volume was dramatically reduced to $^1/_{10^7}$ (from 10 μL to 280 aL) using the extended nanospace channel.

The plate height was not as low as the expected value, but band broadening of the sample zone was nonetheless smaller than the theoretical value during the separation period.[19−21] It was expected that the higher viscosity of the water reduced the diffusion coefficients of the solutes and reduced band broadening during the separation. Band broadening in this study mainly occurred at the time of injection (Figure 4a), and if the sample plug could be injected ideally, the plate height would be less than 0.25 μm.

CONCLUSIONS

In this manuscript we demonstrated the separation of solutes in an extended nanospace channel using pressure-driven flow and achieved highly efficient separation. This result shows that the extended nanospace is useful as a separation column. The merits of using the extended nanospace channel are (1) packing material is not required because of the large interfacial area to volume ratio, (2) good reproducibility is achieved due to the absence of packing material in the channel, (3) very small sample volumes are consumed (a few hundred attoliters), (4) the size and shape of the channels are tunable with high-precision top-down processing technology, and (5) low diffusion coefficients and low plate height are derived from the high viscosity of the mobile phase.

The fLC system can control very small liquid volumes precisely and can thus analyze samples which cannot be analyzed using conventional methods. Therefore, it is anticipated that fLC will be applicable to the analysis of single-cell contents and nanomaterial,[22,23] since the volumes of these samples range from femto- to attoliter.

This fLC system will be a useful experimental tool in many research fields as it can evaluate even weak interactions formed repeatedly between the channel surface and the solutes as the solute passes through the column. Moreover, the simple, straight column shape of this fLC system enables easy elucidation of the mechanism of separation, thus helping to clarify chromatographic separation mechanisms in general.[24]

(19) Gaš, B.; Štěedrý, M.; Kenndler, E. *Electrophoresis* **1997**, *18*, 2123–2133.
(20) Bharadwaj, R.; Santiago, J. G.; Mohammadi, B. *Electrophoresis* **2002**, *23*, 2729–2744.
(21) Culbertson, C. T.; Jacobson, S. C.; Ramsey, J. M. *Anal. Chem.* **1998**, *70*, 3781–3789.
(22) Kato, M.; Onda, Y.; Sekimoto, M.; Degawa, M.; Toyo'oka, T. *J. Chromatogr., A* **2009**, *1216*, 8277–8282.
(23) Yamamoto, T.; Murakami, Y.; Motoyanagi, J.; Fukushima, T.; Maruyama, S.; Kato, M. *Anal. Chem.* **2009**, *81*, 7336–7341.
(24) Wiczling, P.; Kaliszan, R. *Anal. Chem.* **2008**, *80*, 7855–7861.

ACKNOWLEDGMENT

This work was supported by a Grant from the Ministry of Education, Culture, Sports, Science and Technology of Japan and the New Energy and Industrial Technology Development Organization of Japan.

Received for review August 5, 2009. Accepted December 1, 2009.

AC9017605